ACS OMEGA

http://pubs.acs.org/journal/acsodf

Article

Effect of Extending the Conjugation of Dye Molecules on the Efficiency and Stability of Dye-Sensitized Solar Cells

Pengjuan Zhou, Bobing Lin, Ran Chen, Zhongwei An,* Xinbing Chen, Qi An, and Pei Chen

Cite This: *ACS Omega* 2021, 6, 30069−30077

Read Online

ACCESS | Metrics & More | Article Recommendations | Supporting Information

ABSTRACT: We designed and synthesized two organic dyes (**A6** and **A10**) for dye-sensitized solar cells (DSSCs) by extending the molecular conjugation strategy. The sensitizer **A10** was constructed by inserting ethene into our previously reported sensitizer **AZ6**. The sensitizer **A6** was obtained by further substituting the hydrogen of ethene with another donor (D) and π-bridge-acceptor (π−A) segment. The UV−vis spectra and J−V curves showed that the dyes **A10** and **A6** could effectively facilitate the light-harvesting and photocurrent densities with respect to **AZ6**. Consequently, the **A10**-based DSSC achieved an enhanced efficiency (8.54%) with a high photocurrent (18.81 mA cm^{-2}). Desorption experiments of dyes adsorbed on TiO_2 showed that compared with the monoanchoring dyes **AZ6** and **A10**, the dianchoring configuration effectively strengthened the affinity of dye **A6** with the photoanode, making it more difficult to leach from the photoanode. The **A6**-based DSSC shows outstanding stability, and its overall efficiency could remain 98.0% of its initial value after 3000 h of aging time, exceeding that of its monoanalogue **AZ6** (remained 78.3% after 3000 h).

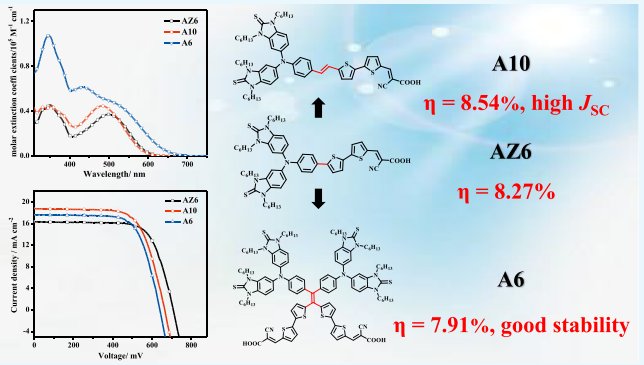

1. INTRODUCTION

Dye-sensitized solar cells, as an ecofriendly and cost-effective photovoltaic device, can efficiently convert both solar and artificial light into electrical energy.[1−3] A conventional DSSC is comprised of a dye-coated photoanode, a counter electrode, and an electrolyte.[4] Sensitizers play an essential role in capturing light and converting it into photocurrent as well as affecting the device stability.[5,6] Zinc porphyrin and ruthenium complexes are typically utilized as sensitizers in DSSCs and exhibit high conversion efficiencies.[7,8] In recent years, metal-free organic dyes have attracted considerable attention because of their tunable light absorption properties, sustainability, and versatile structural modification.[9−11]

In recent decades, many efforts have been focused on developing photosensitizers with broad absorption characteristics, especially in the near-infrared regions.[12,13] One of the promising strategies is to introduce vinyl groups[14−16] or alkynyl groups[17,18] in the π-spacer segment. Relevant studies[19] have shown that inserting vinyl into the dye is a double-edged sword, which generally brings a certain degree of voltage drop but can effectively improve the photocurrent due to better planarity. Our previous report[20] verified that compared with the dye **AZ261**, the dye **AZ263** with an additional vinyl group obtained improved efficiency.

In addition to the traditional D−π−A framework,[21,22] some dianchoring dyes, including the D−(π−A)$_2$,[23−26] double D−π−A, and so forth,[27−32] have also been synthesized. Previous results confirmed that sensitizers featured with a double D−π−A configuration could improve the efficiency and stability of solar cells due to bulky conjugation segments and dual electron injection channels. For example, the dianchoring dyes **LI-57**[33] and **FNE92**[34] gained higher photocurrent compared to the analogue dyes with one anchor group.

In addition to efficiency, long-term stability is an essential prerequisite for DSSC applications.[35] The leakage of electrolytes and unsuitable loading may affect the durability of DSSCs significantly.[36] Compared with DSSCs containing iodine liquid electrolytes,[37,38] DSSCs containing low-volatile electrolytes such as ionic liquid electrolytes,[39−41] quasi-solid electrolytes, and so forth[42−44] have good long-term stability, but their efficiency is generally lower. Recent research shows that the dyes containing dianchoring groups could effectively strengthen the stabilization of dyes, making it more difficult to leach from the photoanode.[45] Furthermore, Grätzel et al. and Su et al. revealed that the dianchoring dyes **DB-1**[46] and **CYF-2**[47] delivered both higher electron injection efficiency and better

Received: August 31, 2021
Accepted: October 19, 2021
Published: October 27, 2021

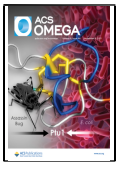

© 2021 The Authors. Published by American Chemical Society

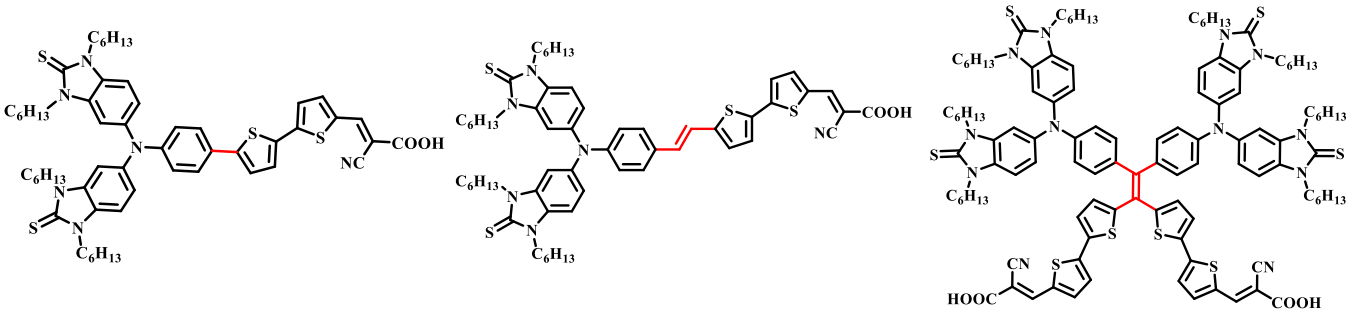

Figure 1. Chemical structures of the dyes.

stability than the monoanchoring dyes **D5** and **CYF-1**, respectively.

It is a normal sense that large conjugation molecules will result in a serious π aggregation in the sensitizers. Our previous reports[48−50] indicated that the cyclic thiourea-functionalized triphenylamine is effective to inhibit the random aggregation of dyes and aims to achieve high efficiency and stability of DSSCs by extending the molecular conjugation. Under the above background, we designed and synthesized the sensitizer **A10**, inserted ethene into our previous dye **AZ6**, and further extended the conjugation to gain sensitizer **A6** by substituting the hydrogen of ethene with another donor (D) and π−A segment (Figure 1). We systematically investigated the photophysical, electrochemistry, photovoltaics, and durability properties to study the structure−performance intrinsic correlation. The results show that the photocurrent can be effectively increased by extending the conjugation of the dyes. The **A10**-based DSSC gained a higher power conversion efficiency (PCE = 8.54%) relying on a higher photocurrent (18.81 mA cm^{-2}) in comparison to **AZ6** (PCE = 8.27%). With the further expansion of molecular conjugation, the **A6**-based DSSC showed good long-term stability, which could remain 98.0% of its initial value after 3000 h of aging time, exceeding that of the monoanalogue **AZ6** (remain 78.3% after 3000 h).

2. RESULTS AND DISCUSSION

2.1. Synthesis. The synthetic routes of sensitizers **A10** and **A6** are shown in Scheme 1. The key compounds **2** and **3** were prepared according to our previous work.[48] Intermediate **2d** was synthesized by Vilsmeier−Haack reaction. Compound **2e** was prepared from compound **2d** by Wittig−Horner reaction and then converted to the corresponding aldehyde **2f** through Bouveault aldehyde synthesis reaction. Intermediate **3n** was obtained through Suzuki cross-coupling of compound **3** with compound **3m**. The dyes **A10** and **A6** were synthesized by the Knoevenagel condensation. All chemical compounds were characterized by ^{1}H NMR, ^{13}C NMR spectroscopy, mass spectroscopy, and infrared spectroscopy.

2.2. UV−Vis Absorption Properties. Figure 2 shows the UV−vis spectra of dyes **AZ6**, **A10**, and **A6** in dichloromethane solution and on the TiO_2 thin film. The corresponding data are listed in Table 1. All dyes exhibited two absorption bands in 310−670 nm regions, respectively. The absorption band in 310−400 nm is assigned to the π−π^* electron transitions, and the latter in 400−670 nm corresponds to the intramolecular charge transfer (ICT) from the donor to the acceptor. **AZ6** and **A10** showed similar absorption curves. However, the dye **A10** exhibited a higher molar extinction coefficient (ε) in the range 380−500 nm due to the extension of π-conjugation and good planarity. We noted that the molar extinction coefficient of **A6** at λ_{max} (345 nm) was very high, reaching up to 10.7 × 10^4 M^{-1} cm^{-1}. At the same time, **A6** showed a shoulder peak at 484 nm, and the tail of its absorption spectra extended up to 680 nm. The molar extinction coefficient of the ICT electron transition band at λ_{max} increases from **AZ6** (3.69 × 10^4 M^{-1} cm^{-1}) to **A10** (4.46 × 10^4 M^{-1} cm^{-1}) to **A6** (6.11 × 10^4 M^{-1} cm^{-1}). Obviously, along with the further extension of conjugation, the absorption band of **A6** is more intense and broader than those of **AZ6** and **A10**.

Upon anchoring on the TiO_2 film, all dyes exhibited broader and red-shifted absorption characteristics. The phenomenon may result from the J-aggregation.[51] The spectra of dyes on TiO_2 films show a complicated trend with respect to those in solutions. **A10** showed the broadest absorption band, indicating a better light-harvesting ability. In order to understand the effect of the structure and size of the dye molecule on the loading capacity, the loading amount of dyes **AZ6**, **A10**, and **A6** was measured, and the corresponding data were 0.84 × 10^{-7} mol cm^{-2}, 0.72 × 10^{-7} mol cm^{-2}, and 0.51 × 10^{-7} mol cm^{-2}, respectively. The dyes **A10** and **AZ6** have similar molecular sizes but different loading capacities, indicating that the inherent structural characteristics of the dyes have an impact on their loading characteristics.[52] The poor loading capacity of **A6** may be caused by multiple factors.[28,34] On the one hand, the large molecular size of **A6** is not conducive to its loading on the TiO_2 surface. On the other hand, the number of anchor groups[53] and the spatial structure characteristics of the two anchors may also affect its dye loading capacity.

To reveal the binding mode of the dye **A6** on TiO_2, FT-IR analysis was performed (Figure S3).[30] The result showed that the characteristic peak of −COOH (1721 cm^{-1}) disappeared, while the characteristic asymmetric stretching (υ_{as}, 1598 cm^{-1}) and symmetric stretching (υ_{s},1408 cm^{-1}) bands of carboxylate units appeared. The results indicated that dye **A6** was absorbed on the TiO_2 surface by the bidentate adsorption mode. We also evaluated the affinity of dyes to TiO_2 by the leaching of the dye in alkaline solution[23] (Figures S4−S5). The result showed that the dye **A6** was more difficult to extract than the monoanchoring dyes, which may benefit the stability of DSSCs.

2.3. Electrochemical Properties. Cyclic voltammetry (CV) was carried out to evaluate the electron injection and dye regeneration process.[54] Figure 3b shows that the highest

https://doi.org/10.1021/acsomega.1c04794
ACS Omega 2021, 6, 30069−30077

Scheme 1. Synthetic Routes of A10, A6[a]

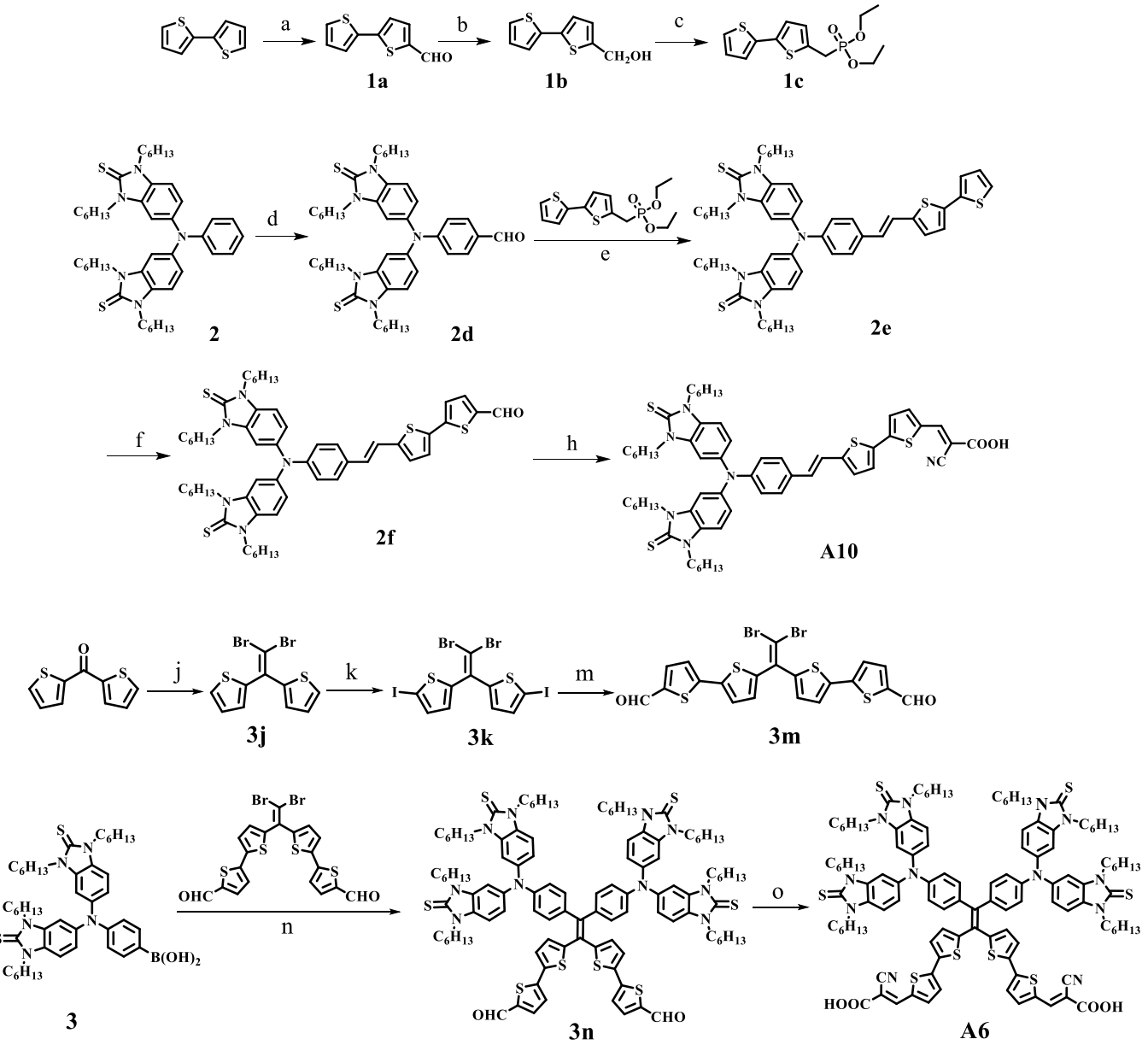

[a]Reaction conditions: (a) $POCl_3$, DMF, DCE, 85 °C, 6 h; (b) $NaBH_4$, CH_3OH, rt, overnight; (c) triethyl phosphite, $ZnBr_2$, rt, 5 h; (d) $POCl_3$, DMF, DCE, 80 °C, 5 h; (e) NaH, THF, rt, overnight; (f) *n*-BuLi, DMF, −78 °C, 2 h; (h) cyanoacetic acid, piperidine, $CHCl_3$, reflux, 3 h; (j) PPh_3, CBr_4, toluene, 140 °C, 24 h; (k) NIS, *p*-TsOH, EtOH, 50 °C, 10 min; (m) $Pd(OAc)_2$, NaF, TBAB, DMF/H_2O, 60 °C, 5 h; (n) K_2CO_3, $Pd(PPh_3)_4$, TBAB, DMF, 75 °C 4 h; (o) cyanoacetic acid, piperidine, $CHCl_3$, reflux, 5 h.

occupied molecular orbital (HOMO) levels of these dyes are lower than the standard potential of iodine redox couples (−4.80 eV vs vacuum), indicating that the dye regeneration process is feasible. Meanwhile, the lowest unoccupied molecular orbital (LUMO) levels of three dyes are more positive than the conduction band (CB) of TiO_2 (−4.0 eV vs vacuum), indicating that the electron injection from the excited dye molecules into TiO_2 has sufficient driving force. The narrow HOMO−LUMO energy gap of **A6** results in a broad spectral response, which is in line with the absorption characteristics in the solution.

2.4. Theoretical Calculation. To get an insight into the optimized geometries and electron distribution of the dyes, the density functional theory (DFT) calculation was performed at the B3LYP/6-311G (d, p) level with the Gaussian 09 program package. The frontier molecular orbitals of the sensitizers and the corresponding energy levels are summarized in Figure 4 and Table S2. Most of the HOMO energy levels of the dye molecules are delocalized on the electron-donating unit and spread to the thiophene unit, while the LUMO and LUMO + 1 levels are primarily distributed on cyanoacrylic acid and extend to the π-spacer segment. The well-overlapped HOMO−LUMO orbitals provide a channel for rapid ICT. For sensitizer **A10**, the phenyl and thiophene rings are almost in one plane (0.31°) due to the insertion of ethene, which facilitates more intense absorption. Meanwhile, as observed in Figure 4, the alkyl chains of the donor part in the sensitizer **A6** can effectively shield its branch chains, preventing dye aggregation

https://doi.org/10.1021/acsomega.1c04794
ACS Omega 2021, 6, 30069−30077

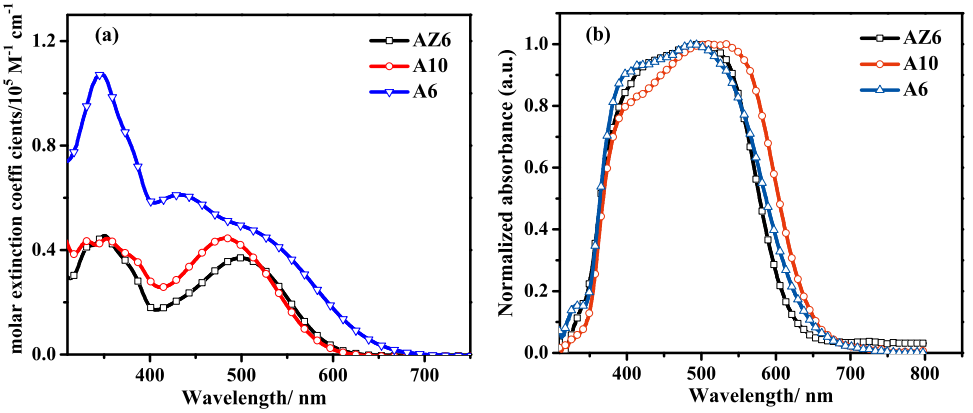

Figure 2. Absorption spectra of dyes **A10**, **A6**, and reference **AZ6** (a) in CH_2Cl_2 solution and (b) normalized absorption spectra on the TiO_2 thin film (thickness: 13 μm) in CH_2Cl_2/t-BuOH (1:1, v/v) solution.

Table 1. Photophysical and Electrochemical Properties of the Dyes

dye	$\lambda_{max/nm}$ ($\varepsilon/10^4$ M^{-1} cm^{-1})[a]	$\lambda_{max/nm}$ ($\varepsilon/10^4$ M^{-1} cm^{-1})[b]	E_{ox} (V)[c]	E_{red} (V)[c]	E_{HOMO} (eV)[c]	E_{LUMO} (eV)[c]	E_g (eV)[c]
AZ6	501 (3.69), 357 (4.34)	504 (5.06)	0.31	−1.06	−5.02	−3.65	1.37
A10	483 (4.46), 357 (4.38)	508 (4.86)	0.29	−1.06	−5.00	−3.65	1.35
A6	432 (6.11), 484 (5.13), 345 (10.70)	491 (4.88)	0.21	−0.99	−4.92	−3.72	1.20

[a]In CH_2Cl_2 solution. [b]On TiO_2 films. [c]$E_{HOMO} = -e(E_{ox} + 4.71)$ (eV), $E_{LUMO} = -e(E_{red} + 4.71)$ (eV); and $E_g = e(E_{ox} - E_{red})$ (eV).

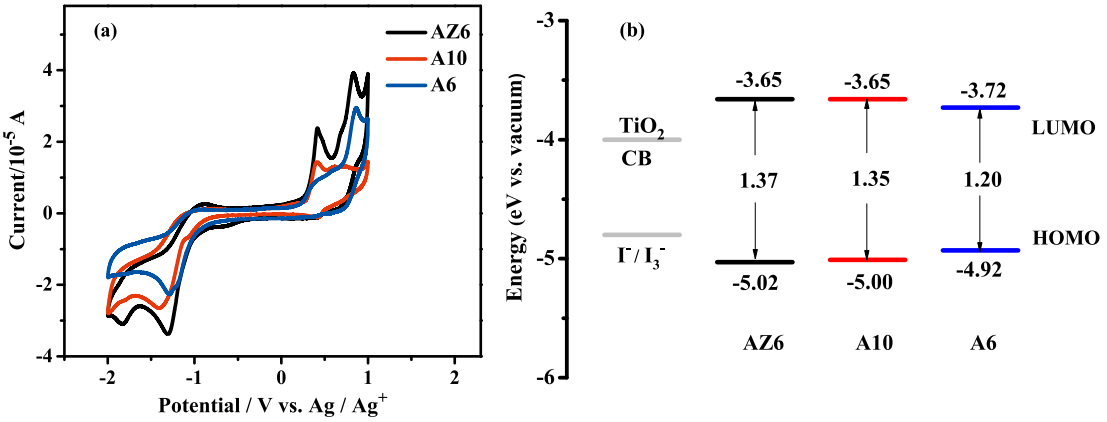

Figure 3. Cyclic voltammograms of dyes (a) in a CH_3CN/CH_2Cl_2 solution and (b) CV-derived energy level diagram of the dyes **AZ6**, **A10**, and **A6**.

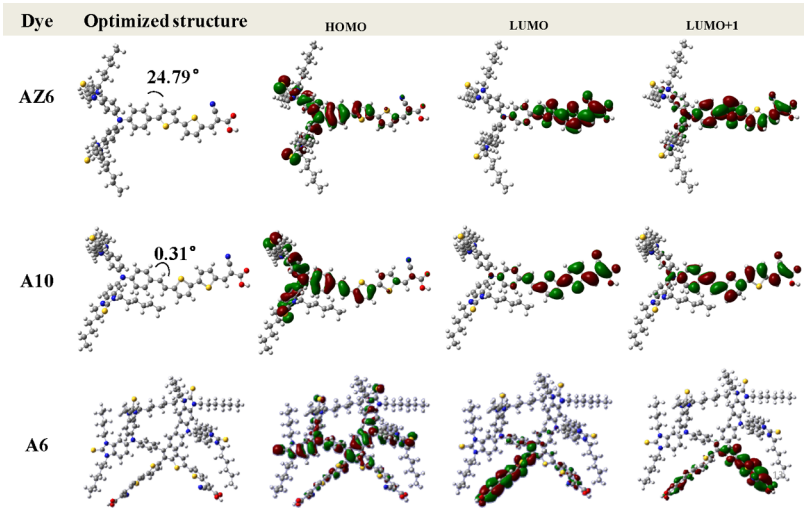

Figure 4. Frontier molecular orbitals and optimized geometry of the dyes **AZ6**, **A10**, and **A6**.

https://doi.org/10.1021/acsomega.1c04794
ACS Omega 2021, 6, 30069−30077

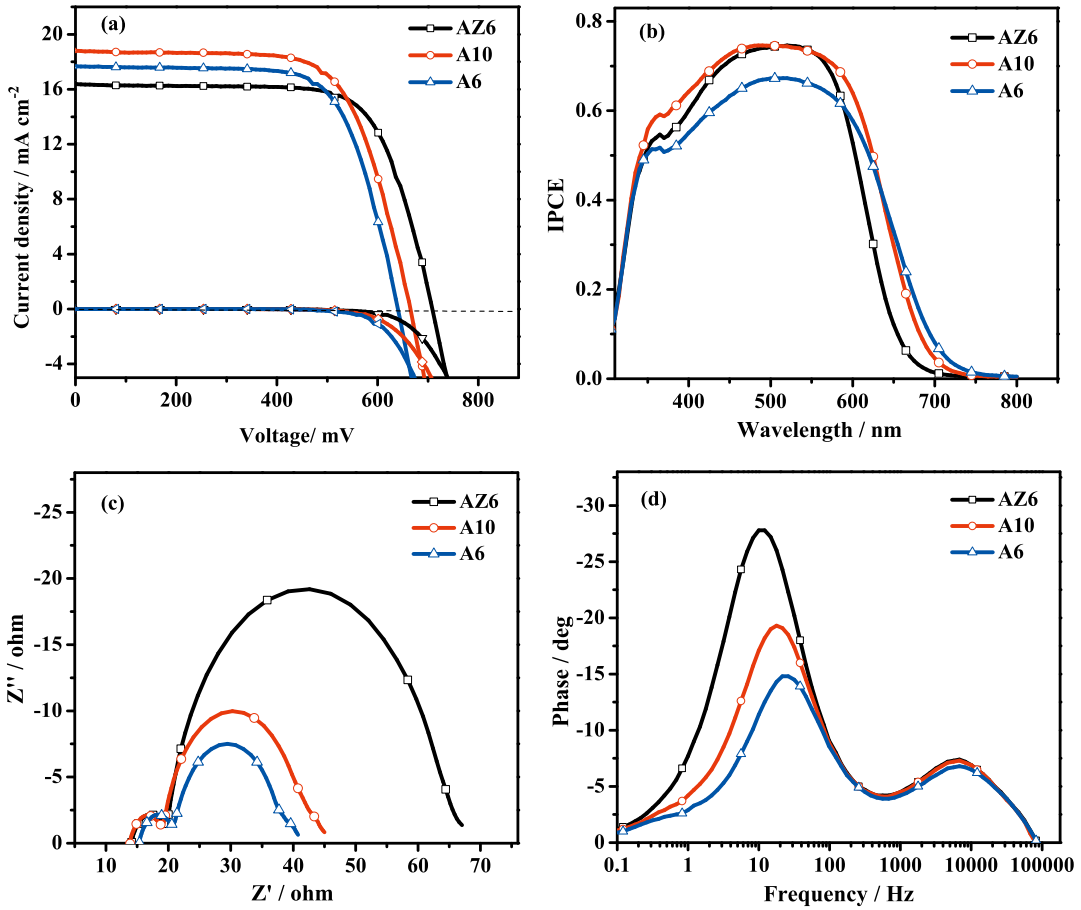

Figure 5. Device performance of the DSSCs based on sensitizers **AZ6**, **A10**, and **A6**: (a) $J-V$ curves, (b) IPCE spectra and EIS spectra, and (c) Nyquist and (d) Bode plots.

Table 2. Photovoltaic Performance of the DSSCs Based on AZ6, A10, and A6[a]

dye	J_{SC} (mA cm^{-2})	V_{OC} (mV)	FF	PCE (%)
AZ6	16.34 (16.84 ± 0.50)	709.2 (689.0 ± 20.2)	0.71 (0.71 ± 0.02)	8.27 (8.24 ± 0.27)
A10	18.81 (18.83 ± 0.27)	664.9 (667.1 ± 9.4)	0.68 (0.67 ± 0.01)	8.54 (8.45 ± 0.13)
A6	17.70 (18.11 ± 0.96)	641.2 (648.2 ± 7.5)	0.70 (0.69 ± 0.01)	7.91 (8.08 ± 0.32)

[a]TiO_2 thickness is 13 μm and the working area is 0.25 cm^2; the averaged photovoltaic parameters of the cells are provided by six parallel cells.

and blocking the oxidized electrolytes from approaching the branch. However, the bulky geometry of **A6** may be detrimental to the dye loading on the TiO_2 surface. The HOMO−LUMO gap values are consistent with the trend of the experimental results of CV.

2.5. Photovoltaic Properties. The photocurrent density−voltage ($J-V$) curves of DSSCs based on the **AZ6**, **A10**, and **A6** dyes are shown in Figure 5. The DSSC performance data are summarized in Table 2. The short-circuit photocurrent density (J_{SC}), open-circuit voltage (V_{OC}), and fill factor (FF) of the **AZ6**-based DSSC are 16.34 mA cm^{-2}, 709.2 mV, and 0.71, respectively, yielding an efficiency of 8.27%. Under the same condition, the **A10**-based DSSC showed an improved efficiency of 8.54% with a J_{SC} of 18.81 mA cm^{-2} and a V_{OC} of 664.9 mV. The higher J_{SC} value of **A10** benefits from the good light absorption observed in Figure 2b. At the same time, the ethene group of **A10** is susceptible to isomerization upon irradiation, leading to serious energy loss in the form of vibration.[55] In addition, compared to **AZ6** (0.84×10^{-7} mol cm^{-2}), the inferior loading amount (0.72×10^{-7} mol cm^{-2}) is unfavorable for the formation of a compact sensitizer layer on the TiO_2 surface, causing undesired dark current. All of the above factors resulted in a low V_{OC} of **A10**. The **A6**-based DSSC attained a lower efficiency of 7.91% due to the low V_{OC} (641.2 mV). Compared with monoanchoring **AZ6** (0.84×10^{-7} mol cm^{-2}) and **A10** (0.72×10^{-7} mol cm^{-2}), **A6** released more protons ($2 \times 0.51 \times 10^{-7}$ mol cm^{-2}) to the TiO_2 film, which caused a shift of the CB (E_{CB}) of TiO_2, resulting in a decreased V_{OC}.[34,56]

The incident photon-to-current conversion efficiency (IPCE) spectra of DSSCs based on these dyes were recorded to elucidate the different J_{SC} values. The IPCE curve of the DSSC based on **A6** showed a bathochromic shift of the ICT band compared to the UV−vis of the dyes on TiO_2 film. Similar phenomena occurred in another report.[42] To clarify this phenomenon, we immersed the sensitized photoanode into the electrolyte for a few seconds and then measured the UV−vis absorption spectra (Figure S6). The results show that the spectral response range of the electrolyte-treated dyes adsorbed on TiO_2 becomes wider. It is worthy to note that **A6**

https://doi.org/10.1021/acsomega.1c04794
ACS Omega 2021, 6, 30069−30077

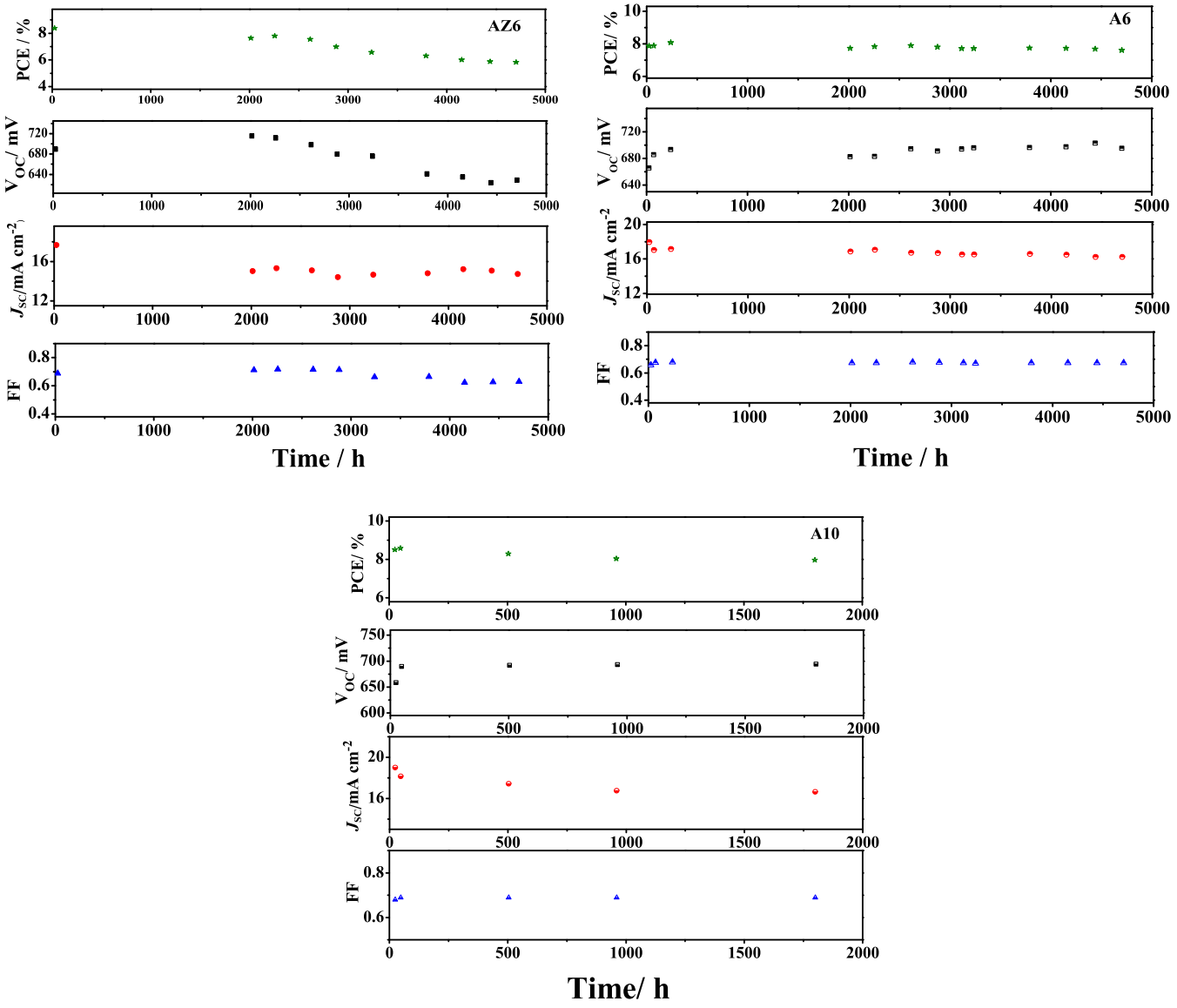

Figure 6. Evaluation of photovoltaic performance parameters for the devices based on **AZ6**, **A10**, and **A6** using the iodide electrolyte under AM 1.5G light soaking.

shows a bathochromic shift of the ICT band and obtains the widest spectra response, indicating more interaction between the dianchoring dye **A6** and the electrolyte. This phenomenon may be related to the molecular structure of the dye **A6**.[24,44] The absorption characteristics are consistent with the IPCE curves. Generally, the integration and intensity of the IPCE spectrum of the dye are consistent with the trend of the J_{SC} value. As shown in Figure 5b, the integration of IPCE is in the order, **AZ6** < **A6** < **A10**, which is consistent with the J_{SC} values.

Long-term stability is of equal importance for DSSC applications. To reveal the difference in photovoltaic performance between the dianchoring dye and the monoanchoring dye, we also evaluated the long-term stability of DSSCs based on the sensitizers. The cells are kept in a dark place, and the relative humidity is controlled around 25%. As shown in Figure 6, the J_{SC}, V_{OC}, FF, and PCE parameters of the cells were recorded over a period of 3000 h under continuous light irradiation (AM 1.5G, 100 mW cm^{-2}). The efficiency of DSSCs based on **A6** and **AZ6** could still maintain 98.2 and 91.0% of their initial values after 2000 h of light soaking, respectively. After 3000 h of light soaking, the efficiency of the **A6**-based DSSC could remain 98.0% of its initial value. However, the efficiency of the **AZ6**-based DSSC could only remain 78.3% of its initial value. The efficiency of the **A10**-based DSSC could remain 93% of its initial value after 1800 h of aging time. The better stability of **A6**-based DSSC may result from the following factors. First, the alkyl chains of the donor unit in the sensitizer **A6** can effectively cover its branch chains, reducing the interaction between the branch and the oxidized electrolytes. Second, according to the experiment results of dyes leaching in an alkaline solution, the bidentate binding mode strengthens the affinity of the dyes on the TiO_2 film and makes it more difficult to leach from the photoanode.

2.6. Electrochemical Impedance Spectroscopy. To investigate the interfacial charge transfer kinetics of DSSCs, electrochemical impedance spectroscopy (EIS) measurements of the DSSCs were carried out. The Nyquist plots and the Bode phase plots are shown in Figure 5. The Nyquist plots present two semicircles, and the larger semicircle corresponds to the recombination resistance. The radius of the larger

https://doi.org/10.1021/acsomega.1c04794
ACS Omega 2021, 6, 30069−30077

semicircle increased in the order **A6** < **A10** < **AZ6**. In Bode plots, the electron recombination lifetime (τ_e) was calculated by the equation $\tau_e = 1/(2\pi f_{max})$. The calculated results increased in the sequence **A6** (6.7 ms) < **A10** (8.9 ms) < **AZ6** (14.7 ms). The larger radius and longer lifetime mean less charge recombination, and these results are consistent with the trend of V_{OC} and dark current.

3. CONCLUSIONS

Two new organic sensitizers **A10** and **A6** were synthesized. The effects of molecular configuration on photophysical, electrochemical, and DSSC performances were systematically studied. By extending the conjugation of dye molecules, the sensitizers **A10** and **A6** generated higher J_{SC} values than the reference sensitizer **AZ6**. The DSSC based on **A10** obtained an improved efficiency (8.54%). Compared with **AZ6**, the **A6** achieved a lower efficiency (7.91%) but much better stability, which can remain at 98.0% of the initial value under continuous light illumination (AM 1.5G, 100 mW cm^{-2}) after 3000 h. The lower V_{OC} value limited the efficiency of **A6**, which may result from the fact that more protons released from the double D−π−A sensitizer **A6**, lowering the Fermi level of TiO_2 and resulting in a low V_{OC}. Combining the efficiency and stability of DSSCs, **A6** is a promising candidate for DSSCs.

4. EXPERIMENTAL SECTION

4.1. Materials and Regents. The chemical reagents and solvents were available from commercial suppliers and used without further purification. The solvents (toluene and tetrahydrofuran) were dried and distilled from sodium under a nitrogen atmosphere.

4.2. Characterization. ^1H NMR and ^{13}C NMR spectra were acquired by 400 MHz (JEOL) or 600 MHz spectrometers (Bruker). The measurements of UV−vis, CV, *J*−*V*, IPCE, and EIS are described in detail in the literature we reported.[57]

4.3. Fabrication of DSSCs. The fluorine-doped SnO_2 conducting glass was cleaned according to our previous reported method.[48] Anatase TiO_2 photoanode (thickness: 13 μm, work area: 0.25 cm^2) was immersed into a 0.4 mM (**AZ6**, **A10**) or 0.3 mM (**A6**) dye bath for 6 h under the dark condition. The iodine liquid electrolyte contains 0.12 M iodine, 1.0 M 1,2-dimethyl-3-propylimidazolium iodide, 0.1 M lithium iodide, and 0.5 M 4-*tert*-butylpyridine, which were dissolved in a mixed solution (CH_3CN/3-methoxypropionitrile = 1:3, v/v). Other processes for the DSSC assembly were performed according to our reported literature earlier.[57]

ASSOCIATED CONTENT

Supporting Information

The Supporting Information is available free of charge at https://pubs.acs.org/doi/10.1021/acsomega.1c04794.

Synthesis and characterization details for the dyes; ^1H NMR, ^{13}C NMR, and mass spectra; loading capacity measurement; FT-IR analysis; desorption experiment; UV−vis of electrolyte-treated dyes on TiO_2; and parameters of the DFT (PDF)

AUTHOR INFORMATION

Corresponding Author

Zhongwei An − *Key Laboratory of Applied Surface and Colloid Chemistry, School of Materials Science and Engineering, Shannxi Normal University, Xi'an 710062, China; Xi'an Modern Chemistry Research Institute, Xi'an 710065, China;* orcid.org/0000-0003-0164-3836; Email: gmecazw@163.com

Authors

Pengjuan Zhou − *Key Laboratory of Applied Surface and Colloid Chemistry, School of Materials Science and Engineering, Shannxi Normal University, Xi'an 710062, China*

Bobing Lin − *Key Laboratory of Applied Surface and Colloid Chemistry, School of Materials Science and Engineering, Shannxi Normal University, Xi'an 710062, China*

Ran Chen − *Key Laboratory of Applied Surface and Colloid Chemistry, School of Materials Science and Engineering, Shannxi Normal University, Xi'an 710062, China*

Xinbing Chen − *Key Laboratory of Applied Surface and Colloid Chemistry, School of Materials Science and Engineering, Shannxi Normal University, Xi'an 710062, China*

Qi An − *North Institute of Scientific and Technical Information, Beijing 100089, China*

Pei Chen − *Key Laboratory of Applied Surface and Colloid Chemistry, School of Materials Science and Engineering, Shannxi Normal University, Xi'an 710062, China;* orcid.org/0000-0002-4317-3361

Complete contact information is available at: https://pubs.acs.org/10.1021/acsomega.1c04794

Notes

The authors declare no competing financial interest.

ACKNOWLEDGMENTS

We are grateful to the financial support by the National Science Foundation Committee of China (21673134 and 21543012), the Program for Science & Technology Innovation Team of Shaanxi Province (2018TD-030), the International Science and Technology Cooperation Project of Shaanxi Province (2021KW-20), and the Fundamental Research Funds for the Central Universities (GK202101005).

REFERENCES

(1) Reddy, K. S. K.; Liu, Y.-C.; Chou, H.-H.; Kala, K.; Wei, T.-C.; Yeh, C.-Y. Synthesis and Characterization of Novel β-Bis(N,N-diarylamino)-Substituted Porphyrin for Dye-Sensitized Solar Cells under 1 sun and Dim Light Conditions. *ACS Appl. Mater. Interfaces* **2018**, *10*, 39970−39982.

(2) Tingare, Y. S.; Vinh, N. S. n.; Chou, H.-H.; Liu, Y.-C.; Long, Y.-S.; Wu, T.-C.; Wei, T.-C.; Yeh, C.-Y. New Acetylene-Bridged 9,10-Conjugated Anthracene Sensitizers: Application in Outdoor and Indoor Dye-Sensitized Solar Cells. *Adv. Energy Mater.* **2017**, *7*, 1700032.

(3) Zhou, N.; Prabakaran, K.; Lee, B.; Chang, S. H.; Harutyunyan, B.; Guo, P.; Butler, M. R.; Timalsina, A.; Bedzyk, M. J.; Ratner, M. A.; Vegiraju, S.; Yau, S.; Wu, C.-G.; Chang, R. P. H.; Facchetti, A.; Chen, M.-C.; Marks, T. J. Metal-Free Tetrathienoacene Sensitizers for High-Performance Dye-Sensitized Solar Cells. *J. Am. Chem. Soc.* **2015**, *137*, 4414−4423.

(4) Chen, Y.-C.; Lin, J. T. Multi-anchored sensitizers for dye-sensitized solar cells. *Sustainable Energy Fuels* **2017**, *1*, 969−985.

(5) Qu, S.; Qin, C.; Islam, A.; Wu, Y.; Zhu, W.; Hua, J.; Tian, H.; Han, L. A novel D-A-π-A organic sensitizer containing a diketopyrrolopyrrole unit with a branched alkyl chain for highly efficient and stable dye-sensitized solar cells. *Chem. Commun.* **2012**, *48*, 6972−6974.
(6) Ying, W.; Yang, J.; Wielopolski, M.; Moehl, T.; Moser, J.-E.; Comte, P.; Hua, J.; Zakeeruddin, S. M.; Tian, H.; Grätzel, M. New pyrido[3,4-b]pyrazine-based sensitizers for efficient and stable dye-sensitized solar cells. *Chem. Sci.* **2014**, *5*, 206−214.
(7) Zhang, S.; Yang, X.; Numata, Y.; Han, L. Highly efficient dye-sensitized solar cells: progress and future challenges. *Energy Environ. Sci.* **2013**, *6*, 1443−1464.
(8) Zou, J.; Yan, Q.; Li, C.; Lu, Y.; Tong, Z.; Xie, Y. Light-Absorbing Pyridine Derivative as a New Electrolyte Additive for Developing Efficient Porphyrin Dye-Sensitized Solar Cells. *ACS Appl. Mater. Interfaces* **2020**, *12*, 57017−57024.
(9) Xu, M.; Hu, X.; Zhang, Y.; Bao, X.; Pang, A.; Fang, J.-K. Novel Organic Dyes Featuring Spiro[dibenzo[3,4:6,7]cyclohepta[1,2-b]-quinoxaline-10,9′-fluorene] (SDBQX) as a Rigid Moiety for Dye-Sensitized Solar Cells. *ACS Appl. Energy Mater.* **2018**, *1*, 2200−2207.
(10) Duvva, N.; Eom, Y. K.; Reddy, G.; Schanze, K. S.; Giribabu, L. Bulky Phenanthroimidazole-Phenothiazine D−π-A Based Organic Sensitizers for Application in Efficient Dye-Sensitized Solar Cells. *ACS Appl. Energy Mater.* **2020**, *3*, 6758−6767.
(11) Chen, Y.-H.; Nguyen, V. S.; Chou, H.-H.; Tingare, Y. S.; Wei, T.-C.; Yeh, C.-Y. Anthracene Organic Sensitizer with Dual Anchors for Efficient and Robust Dye-Sensitized Solar Cells. *ACS Appl. Energy Mater.* **2020**, *3*, 5479−5486.
(12) Wu, Y.; Zhu, W.-H.; Zakeeruddin, S. M.; Grätzel, M. Insight into D-A−π-A Structured Sensitizers: A Promising Route to Highly Efficient and Stable Dye-Sensitized Solar Cells. *ACS Appl. Mater. Interfaces* **2015**, *7*, 9307−9318.
(13) Raju, T. B.; Vaghasiya, J. V.; Afroz, M. A.; Soni, S. S.; Iyer, P. K. Effect of mono- and di-anchoring dyes based on o,m-difluoro substituted phenylene spacer in liquid and solid state dye sensitized solar cells. *Dyes Pigm.* **2020**, *174*, 108021.
(14) Cai, L.; Tsao, H. N.; Zhang, W.; Wang, L.; Xue, Z.; Grätzel, M.; Liu, B. Organic Sensitizers with Bridged Triphenylamine Donor Units for Efficient Dye-Sensitized Solar Cells. *Adv. Energy Mater.* **2013**, *3*, 200−205.
(15) Tian, Z.; Huang, M.; Zhao, B.; Huang, H.; Feng, X.; Nie, Y.; Shen, P.; Tan, S. Low-cost dyes based on methylthiophene for high-performance dye-sensitized solar cells. *Dyes Pigm.* **2010**, *87*, 181−187.
(16) Zhang, L.; Yang, X.; Wang, W.; Gurzadyan, G. G.; Li, J.; Li, X.; An, J.; Yu, Z.; Wang, H.; Cai, B.; Hagfeldt, A.; Sun, L. 13.6% Efficient Organic Dye-Sensitized Solar Cells by Minimizing Energy Losses of the Excited State. *ACS Energy Lett.* **2019**, *4*, 943−951.
(17) Ren, Y.; Li, Y.; Chen, S.; Liu, J.; Zhang, J.; Wang, P. Improving the performance of dye-sensitized solar cells with electron-donor and electron-acceptor characteristic of planar electronic skeletons. *Energy Environ. Sci.* **2016**, *9*, 1390−1399.
(18) Xie, X.; Sun, D.; Wei, Y.; Yuan, Y.; Zhang, J.; Ren, Y.; Wang, P. Thienochrysenocarbazole based organic dyes for transparent solar cells with over 10% efficiency. *J. Mater. Chem. A* **2019**, *7*, 11338−11346.
(19) Liu, J.; Zhou, D.; Xu, M.; Jing, X.; Wang, P. The structure-property relationship of organic dyes in mesoscopic titania solar cells: only one double-bond difference. *Energy Environ. Sci.* **2011**, *4*, 3545−3551.
(20) Zhu, S.; An, Z.; Chen, X.; Chen, P.; Liu, Q. Approach to tune short-circuit current and open-circuit voltage of dye-sensitized solar cells: π-linker modification and photoanode selection. *RSC Adv.* **2014**, *4*, 42252−42259.
(21) Kakiage, K.; Aoyama, Y.; Yano, T.; Oya, K.; Fujisawa, J.-i.; Hanaya, M. Highly-efficient dye-sensitized solar cells with collaborative sensitization by silyl-anchor and carboxy-anchor dyes. *Chem. Commun.* **2015**, *51*, 15894−15897.
(22) Liang, M.; Chen, J. Arylamine organic dyes for dye-sensitized solar cells. *Chem. Soc. Rev.* **2013**, *42*, 3453−3488.
(23) Li, C.-T.; Kuo, Y.-L.; Kumar, C. P.; Huang, P.-T.; Lin, J. T. Tetraphenylethylene tethered phenothiazine-based double-anchored sensitizers for high performance dye-sensitized solar cells. *J. Mater. Chem. A* **2019**, *7*, 23225−23233.
(24) Lee, W.; Yuk, S. B.; Choi, J.; Kim, H. J.; Kim, H. W.; Kim, S. H.; Kim, B.; Ko, M. J.; Kim, J. P. The effects of the number of anchoring groups and N-substitution on the performance of phenoxazine dyes in dye-sensitized solar cells. *Dyes Pigm.* **2014**, *102*, 13−21.
(25) Li, Y.; Song, P.; Yang, Y.; Ma, F.; Li, Y. Double-anchoring organic dyes for dye-sensitized solar cells: the opto-electronic property and performance. *New J. Chem.* **2017**, *41*, 12808−12829.
(26) Manfredi, N.; Cecconi, B.; Abbotto, A. Multi-Branched Multi-Anchoring Metal-Free Dyes for Dye-Sensitized Solar Cells. *Eur. J. Org. Chem.* **2014**, 7069−7086.
(27) Hong, Y.; Liao, J.-Y.; Fu, J.; Kuang, D.-B.; Meier, H.; Su, C.-Y.; Cao, D. Performance of dye-sensitized solar cells based on novel sensitizers bearing asymmetric double D−π−A chains with arylamines as donors. *Dyes Pigm.* **2012**, *94*, 481−489.
(28) Huang, Z.-S.; Cai, C.; Zang, X.-F.; Iqbal, Z.; Zeng, H.; Kuang, D.-B.; Wang, L.; Meier, H.; Cao, D. Effect of the linkage location in double branched organic dyes on the photovoltaic performance of DSSCs. *J. Mater. Chem. A* **2015**, *3*, 1333−1344.
(29) Meier, H.; Huang, Z.-S.; Cao, D. Double D-π-A branched dyes - a new class of metal-free organic dyes for efficient dye-sensitized solar cells. *J. Mater. Chem. C* **2017**, *5*, 9828−9837.
(30) Sil, M. C.; Sudhakar, V.; Mele Kavungathodi, M. F.; Punitharasu, V.; Nithyanandhan, J. Orthogonally Functionalized Donor/Acceptor Homo- and Heterodimeric Dyes for Dye-Sensitized Solar Cells: An Approach to Introduce Panchromaticity and Control the Charge Recombination. *ACS Appl. Mater. Interfaces* **2017**, *9*, 34875−34890.
(31) Zeng, K.; Chen, Y.; Zhu, W.-H.; Tian, H.; Xie, Y. Efficient Solar Cells Based on Concerted Companion Dyes Containing Two Complementary Components: An Alternative Approach for Cosensitization. *J. Am. Chem. Soc.* **2020**, *142*, 5154−5161.
(32) Qian, X.; Gao, H.-H.; Zhu, Y.-Z.; Lu, L.; Zheng, J.-Y. Biindole-based double D-π-A branched organic dyes for efficient dye-sensitized solar cells. *RSC Adv.* **2015**, *5*, 4368−4375.
(33) Li, H.; Hou, Y.; Yang, Y.; Tang, R.; Chen, J.; Wang, H.; Han, H.; Peng, T.; Li, Q.; Li, Z. Attempt to Improve the Performance of Pyrrole-Containing Dyes in Dye Sensitized Solar Cells by Adjusting Isolation Groups. *ACS Appl. Mater. Interfaces* **2013**, *5*, 12469−12477.
(34) Ren, X.; Jiang, S.; Cha, M.; Zhou, G.; Wang, Z.-S. Thiophene-Bridged Double D-π-A Dye for Efficient Dye-Sensitized Solar Cell. *Chem. Mater.* **2012**, *24*, 3493−3499.
(35) Katoh, R.; Furube, A.; Mori, S.; Miyashita, M.; Sunahara, K.; Koumura, N.; Hara, K. Highly stable sensitizer dyes for dye-sensitized solar cells: role of the oligothiophene moiety. *Energy Environ. Sci.* **2009**, *2*, 542−546.
(36) Lu, X.; Jia, X.; Wang, Z.-S.; Zhou, G. X-shaped organic dyes with a quinoxaline bridge for use in dye-sensitized solar cells. *J. Mater. Chem. A* **2013**, *1*, 9697−9706.
(37) Zeng, K.; Lu, Y.; Tang, W.; Zhao, S.; Liu, Q.; Zhu, W.; Tian, H.; Xie, Y. Efficient solar cells sensitized by a promising new type of porphyrin: dye-aggregation suppressed by double strapping. *Chem. Sci.* **2019**, *10*, 2186−2192.
(38) Huang, J.-F.; Liu, J.-M.; Su, P.-Y.; Chen, Y.-F.; Shen, Y.; Xiao, L.-M.; Kuang, D.-B.; Su, C.-Y. Highly efficient and stable cyclometalated ruthenium(II) complexes as sensitizers for dye-sensitized solar cells. *Electrochim. Acta* **2015**, *174*, 494−501.
(39) He, J.; Guo, F.; Li, X.; Wu, W.; Yang, J.; Hua, J. New Bithiazole-Based Sensitizers for Efficient and Stable Dye-Sensitized Solar Cells. *Chem.—Eur. J.* **2012**, *18*, 7903−7915.
(40) Wang, P.; Yang, L.; Wu, H.; Cao, Y.; Zhang, J.; Xu, N.; Chen, S.; Decoppet, J.-D.; Zakeeruddin, S. M.; Grätzel, M. Stable and Efficient Organic Dye-Sensitized Solar Cell Based on Ionic Liquid Electrolyte. *Joule* **2018**, *2*, 2145−2153.

https://doi.org/10.1021/acsomega.1c04794
ACS Omega 2021, 6, 30069−30077

(41) Zhu, W.; Wu, Y.; Wang, S.; Li, W.; Li, X.; Chen, J.; Wang, Z.-s.; Tian, H. Organic D-A-π-A Solar Cell Sensitizers with Improved Stability and Spectral Response. *Adv. Funct. Mater.* **2011**, *21*, 756−763.
(42) Feng, Q.; Jia, X.; Zhou, G.; Wang, Z.-S. Embedding an electron donor or acceptor into naphtho[2,1-b:3,4-b′]dithiophene based organic sensitizers for dye-sensitized solar cells. *Chem. Commun.* **2013**, *49*, 7445−7447.
(43) Feng, Q.; Zhang, Q.; Lu, X.; Wang, H.; Zhou, G.; Wang, Z.-S. Facile and Selective Synthesis of Oligothiophene-Based Sensitizer Isomers: An Approach toward Efficient Dye-Sensitized Solar Cells. *ACS Appl. Mater. Interfaces* **2013**, *5*, 8982−8990.
(44) Lu, X.; Feng, Q.; Lan, T.; Zhou, G.; Wang, Z.-S. Molecular Engineering of Quinoxaline-Based Organic Sensitizers for Highly Efficient and Stable Dye-Sensitized Solar Cells. *Chem. Mater.* **2012**, *24*, 3179−3187.
(45) Hung, W.-I.; Liao, Y.-Y.; Lee, T.-H.; Ting, Y.-C.; Ni, J.-S.; Kao, W.-S.; Lin, J. T.; Wei, T.-C.; Yen, Y.-S. Eugenic metal-free sensitizers with double anchors for high performance dye-sensitized solar cells. *Chem. Commun.* **2015**, *51*, 2152−2155.
(46) Abbotto, A.; Manfredi, N.; Marinzi, C.; De Angelis, F.; Mosconi, E.; Yum, J.-H.; Xianxi, Z.; Nazeeruddin, M. K.; Grätzel, M. Di-branched di-anchoring organic dyes for dye-sensitized solar cells. *Energy Environ. Sci.* **2009**, *2*, 1094−1101.
(47) Chen, Y.-F.; Liu, J.-M.; Huang, J.-F.; Tan, L.-L.; Shen, Y.; Xiao, L.-M.; Kuang, D.-B.; Su, C.-Y. Stable organic dyes based on the benzo[1,2-b:4,5-b′]dithiophene donor for efficient dye-sensitized solar cells. *J. Mater. Chem. A* **2015**, *3*, 8083−8090.
(48) Wu, Z.; An, Z.; Chen, X.; Chen, P. Cyclic Thiourea/Urea Functionalized Triphenylamine-Based Dyes for High-Performance Dye-Sensitized Solar Cells. *Org. Lett.* **2013**, *15*, 1456−1459.
(49) Zhu, S.; An, Z.; Sun, X.; Wu, Z.; Chen, X.; Chen, P. Synthesis and evaluation of simple molecule as a co-adsorbent dye for highly efficient co-sensitized solar cells. *Dyes Pigm.* **2015**, *120*, 85−92.
(50) Liu, S.; Zhou, M.; Zhang, G.; Chen, R.; Zhou, P.; An, Z.; Chen, X.; An, Q.; Chen, P. The effect of benzoxazole unit on the properties of cyclic thiourea functionalized triphenylamine dye sensitizers. *Dyes Pigm.* **2021**, *187*, 109093.
(51) Zhao, Q.; Lai, H.; Chen, H.; Li, H.; He, F. H- and J-aggregation inspiring efficient solar conversion. *J. Mater. Chem. A* **2021**, *9*, 1119−1126.
(52) Lo, C.-Y.; Kumar, D.; Chou, S.-H.; Chen, C.-H.; Tsai, C.-H.; Liu, S.-H.; Chou, P.-T.; Wong, K.-T. Highly Twisted Dianchoring D−π-A Sensitizers for Efficient Dye-Sensitized Solar Cells. *ACS Appl. Mater. Interfaces* **2016**, *8*, 27832−27842.
(53) Wang, X.; Bolag, A.; Yun, W.; Du, Y.; Eerdun, C.; Zhang, X.; Bao, T.; Ning, J.; Alata, H.; Ojiyed, T. Enhanced performance of dye-sensitized solar cells based on a dual anchored diphenylpyranylidene dye and N719 co-sensitization. *J. Mol. Struct.* **2020**, *1206*, 127694.
(54) Hou, J.; Tan, Z.; Yan, Y.; He, Y.; Yang, C.; Li, Y. Synthesis and Photovoltaic Properties of Two-Dimensional Conjugated Polythiophenes with Bi(thienylenevinylene) Side Chains. *J. Am. Chem. Soc.* **2006**, *128*, 4911−4916.
(55) Ning, Z.; Fu, Y.; Tian, H. Improvement of dye-sensitized solar cells: what we know and what we need to know. *Energy Environ. Sci.* **2010**, *3*, 1170−1181.
(56) Li, C.-T.; Wu, F.-L.; Liang, C.-J.; Ho, K.-C.; Lin, J. T. Effective suppression of interfacial charge recombination by a 12-crown-4 substituent on a double-anchored organic sensitizer and rotating disk electrochemical evidence. *J. Mater. Chem. A* **2017**, *5*, 7586−7594.
(57) Zhou, P.; Liang, J.; Lin, B.; An, Z.; Chen, R.; Chen, X.; An, Q.; Chen, P. Effect of the Spatial Configuration of Donors on the Photovoltaic Performance of Double D−π-A Organic Dyes. *ACS Appl. Mater. Interfaces* **2021**, *13*, 40648−40655.

https://doi.org/10.1021/acsomega.1c04794
ACS Omega 2021, 6, 30069−30077